Phase transitions in high-pressure ^{4}He: A study using molecular-dynamics and Monte Carlo methods

D. Levesque and J. J. Weis
Laboratoire de Physique Théorique et Hautes Energies, Université de Paris—Sud, Bâtiment 211, 91405 Orsay, France

P. Loubeyre
Physique des Milieux très Condensés, Université Pierre et Marie Curie, 75230 Paris Cédex 05, France
(Received 5 February 1986)

We determine the latent heats and volume changes of the phase transitions of ^{4}He near 300 K by numerical simulations in the isobaric-isoenthalpic and isothermal-isobaric ensembles. The simulations in these two ensembles which use either the molecular-dynamics or the Monte Carlo method are shown to be of equal efficiency for the study of solid-solid transitions.

I. INTRODUCTION

A triple point between two solid phases and a liquid phase has been evidenced recently in the phase diagram of ^{4}He at 300 K by high-pressure experiments using the diamond-anvil-cell technique.[1] Theoretical studies have identified the structure of the new solid phase at high temperature as being of the bcc type; the low-temperature solid phase is known to be fcc. In these studies two different approaches have been used. In the first one the free energies of the liquid and the solid phases are calculated in order to determine the melting line[1] and the solid-solid transition line.[2,3] The free energies have been evaluated by perturbation theory (liquid phase) and lattice dynamics (solid phase). The second approach[4] resorts to a molecular-dynamics simulation method, proposed by Parrinello and Rahman[5] to obtain the regions of the phase diagram in which the liquid and solid phases are stable. Both approaches are complementary. In fact, for the values of the pressure and density corresponding to the triple point of ^{4}He at 300 K, the validity of the theoretical approximations used in the calculation of the free energies of the different phases can only be established by comparison with "exact" simulation results.

The aim of the present article is to give a precise description of the phase diagram in the vicinity of the triple point at $T \sim 300$ K by determining the volume changes occurring during the transition from the fcc to the bcc phase and during melting. Both molecular-dynamics (MD) simulations at constant enthalpy[5] and Monte Carlo (MC) simulations in the isothermal-isobaric ensemble[6] have been used to determine these volume changes. In the former simulation method, where enthalpy and pressure remain constant during the dynamical evolution of the system, we investigated, at a given pressure, which phase was stable as a function of enthalpy, the volume change at the solid-solid transition was then obtained by determining the temperature at which the two solid phases are in equilibrium. In the MC simulations, where the pressure and temperature are fixed, we studied, for a given temperature, the stability of the solid phases as a function of pressure. In this case, the variation of volume at the transition was obtained for the pressure at which the two phases are in equilibrium.

All our calculations have been performed with the potential proposed by Aziz *et al.*[7] which is known[8] to give an excellent description of the interaction between ^{4}He atoms.

Our article is organized as follows. In Sec. II we present the MD results obtained along two isobars and describe the method used to determine the equilibrium temperature between the two solid phases. In Sec. III we discuss the practical realization of a simulation study of a solid-solid phase change in the isothermal-isobaric ensemble and give the results for the calculations along one isotherm. The latter complement those of Sec. II and show that volume changes in a phase transition are easier obtained by simulations in the isothermal-isobaric ensemble than in the isobaric-isoenthalpic ensemble.

The conclusions are given in Sec. IV. We briefly discuss which types of crystal deformations occur in the fcc-bcc and bcc-fcc transitions.

II. MOLECULAR-DYNAMICS STUDY

The MD method of Parrinello and Rahman[5] which we employed in our study of the solid-solid transition in ^{4}He at high temperature is described in detail in Refs. 9 and 10. It amounts to calculating the evolution of the positions of N atoms in a parallelepipedic box with periodic boundary conditions. The system has variable volume and shape. In fact the lengths and orientations of the basis vectors **a**, **b**, **c** defining the MD cell are a function of the dynamics of the system. The variation of **a**, **b**, and **c** is essential to allow the system to evolve from one solid phase to another. Indeed the unit cell of the different lattices must be compatible with the periodic boundary conditions when the atoms form a perfect crystal arrangement.

In the method of Parrinello and Rahman, the equations of motion of the system follow from the Lagrangian

$$\mathscr{L}=\tfrac{1}{2}\sum_{i=1}^{N} m\dot{\mathbf{s}}_i\cdot\overleftrightarrow{G}\cdot\dot{\mathbf{s}}_i-\sum_{\substack{i,j=1\\(i<j)}}^{N} v(r_{ij})$$
$$+\tfrac{1}{2}W\,\mathrm{Tr}\{\overleftrightarrow{h}^t\cdot\overleftrightarrow{h}\}-P\det\{\overleftrightarrow{h}\}\ , \tag{1}$$

where $\mathbf{r}_i$ is the position of atom i, $v(r_{ij})$ the interaction potential between atoms i and j ($r_{ij}=|\mathbf{r}_i-\mathbf{r}_j|$). The components s_i^α of the vector $\mathbf{s}_i$ are related to those of $\mathbf{r}_i$ through the relation $r_i^\alpha=\sum h_{\alpha\beta}s_i^\beta$, where $a^\alpha=h_{1\alpha}$, $b^\alpha=h_{2\alpha}$, and $c^\alpha=h_{3\alpha}$. The volume V at instant t is $V=\det\{\overleftrightarrow{h}\}$, $\overleftrightarrow{h}^t$ denotes the transpose of h, and $G_{\alpha\beta}=\sum_\gamma h'_{\alpha\gamma}h_{\gamma\beta}$. W is a parameter and P the thermodynamic pressure of the system.

In fact, the Hamiltonian associated with $\mathscr{L}$ is

$$H=\tfrac{1}{2}\sum_{i=1}^{N} m\dot{\mathbf{s}}_i\cdot\overleftrightarrow{G}\cdot\dot{\mathbf{s}}_i+\sum_{i(<j)=1}^{N} v(r_{ij})$$
$$+\tfrac{1}{2}W\,\mathrm{Tr}\{\overleftrightarrow{h}^t\cdot\overleftrightarrow{h}\}+P\det\{\overleftrightarrow{h}\}\ . \tag{2}$$

Taking the average value of the right-hand side of (2) over time one obtains

$$H=\left\langle\tfrac{1}{2}\sum_{i=1}^{N} m\dot{\mathbf{s}}_i\cdot\overleftrightarrow{G}\cdot\dot{\mathbf{s}}_i+\tfrac{1}{2}W\,\mathrm{Tr}\{\overleftrightarrow{h}^t\cdot\overleftrightarrow{h}\}\right\rangle+U+P\overline{V}$$

with $\overline{V}=\langle\det\{\overleftrightarrow{h}\}\rangle$, $U=\langle\sum_{i<j=1}^{N}v(r_{ij})\rangle$. The temperature of the system is defined as

$$T=\left\langle\sum_{i=1}^{N} m\dot{\mathbf{s}}_i\cdot\overleftrightarrow{G}\cdot\dot{\mathbf{s}}_i+W\,\mathrm{Tr}\{\overleftrightarrow{h}^t\cdot\overleftrightarrow{h}\}\right\rangle\Big/(3N+9)k_B\ , \tag{3}$$

where k_B is the Boltzmann constant. For sufficiently large N the term $\langle W\,\mathrm{Tr}\{\overleftrightarrow{h}^t\cdot\overleftrightarrow{h}\}\rangle$ corresponding to a kinetic energy of $9k_BT$ becomes negligible so that H can be identified with the enthalpy of the system, as $\overline{V}$ is the mean volume and P is the pressure. The average over the time evolution of the system corresponds, H being conserved, to an average in the isobaric-isoenthalpic ensemble to which can be associated a canonical isothermal-isobaric ensemble.[11] From the initial conditions $[\mathbf{s}_i(0),\dot{\mathbf{s}}_i(0),\overleftrightarrow{h}(0),\dot{\overleftrightarrow{h}}(0)]$ the evolution of the system occurs in the $(6N+18)$-dimensional space on a surface corresponding to constant H. The trajectory followed on this surface is a succession of equiprobable states belonging eventually to different phases (liquid, fcc, bcc). It is thus essential to be able to identify these phases. In our work the identification of the phase, in which the system is at time t, is achieved by means of the function $g_n(r)$ defined in the following way: Over an interval of n time steps of integration of the equations of motion, one calculates the mean volume V_n and the mean number of atoms $N_n(r)$ at a distance between r and $r+dr$ from an atom; $g_n(r)$ is then given by

$$g_n(r)=\frac{N_n(r)V_n}{4\pi r^2 dr\,N}\ . \tag{4}$$

For a system in the liquid state $g_n(r)$ is proportional to the two-body correlation function $\rho^{(2)}(\mathbf{r}_1,\mathbf{r}_2)$, and in the solid state proportional to the average of $\rho^{(2)}(\mathbf{r}_1,\mathbf{r}_2)$ over all orientations of the vector $\mathbf{r}=\mathbf{r}_2-\mathbf{r}_1$. Figure 1 shows the variation of $g_n(r)$ for $n=50$ in the fcc, bcc, and liquid phases of a system of 432 atoms interacting via the potential of Aziz *et al.*[7] at density $\rho^*=\rho\sigma^3\sim2.4$ and temperature $T^*=k_BT/\epsilon=35$ ($\epsilon/k_B=10.22$ K, $\sigma=2.552$ Å). As the values of ρ^* and T^* are very high (respectively, 2.5 and 50 times those of argon near its triple point) the positions of the different shells of neighbors are not easily identified in the solid phases, in particular the two first shells are mingled in the first peak of $g_n(r)$. However, there is a marked qualitative difference between the functions $g_n(r)$ of the three phases. For the fcc and bcc phases the numbers of neighbors in the 7 first shells are 12,6,24,12,24,8,48,6 and 8,6,12,24,8,6,24,24, respectively. The small number of atoms in the fifth and sixth shells of the bcc structure gives a pronounced minimum in $g_n(r)$ at a distance $\sim1.8\sigma$; the difference of the number of atoms in the third and fourth shells of the fcc and bcc lattices manifests itself in the relative heights of the maxima of $g_n(r)$ at $r=1.48\sigma$ and 1.56σ. The liquid phase is readily identified by a damped oscillating behavior of $g_n(r)$ with period of about σ. As already shown in Ref. 4 it is thus easily possible, if a phase change occurs, to follow the evolution of the system from one phase to another by simple inspection of $g_n(r)$ calculated for $n\approx50$.

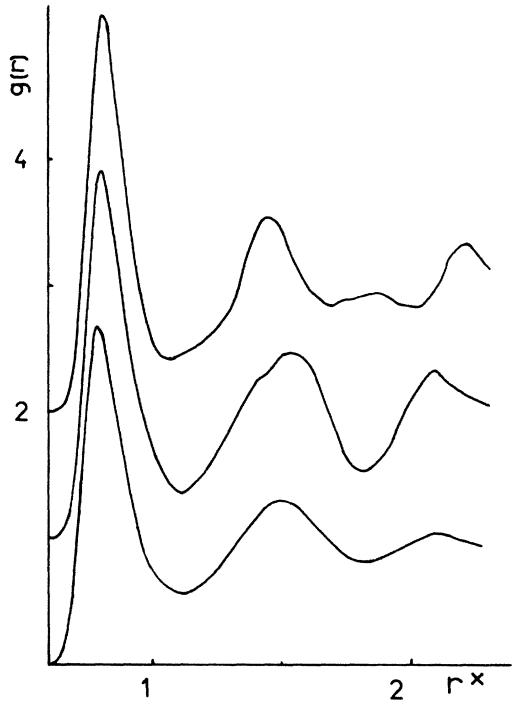

FIG. 1. From bottom to top, pair correlation functions $g_n(r)$ for the liquid phase ($\rho^*=2.349$, $T^*=36$), the bcc phase ($\rho^*=2.398$, $T^*=36.3$), and the fcc phase ($\rho^*=2.394$, $T^*=34.4$). n is equal to 50.

The passage from one phase to another may be accompanied by defects in the atomic arrangements. However, one can verify that for the densities and temperatures considered here, defects, if occurring at all, do not modify no-

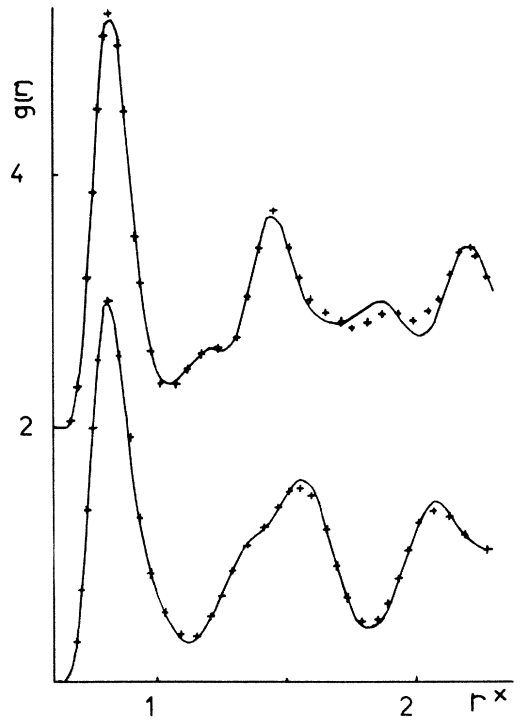

FIG. 2. Comparison between the $g(r)$'s calculated by MD simulations at constant energy and fixed volume (solid line) and at constant enthalpy and fixed pressure (crosses) (top: fcc phase, bottom: bcc phase). The $g(r)$'s at fixed volume were computed from an average over 500 time steps at $\rho^*=2.409$, $T^*=31.9$ (bcc) and $\rho^*=2.414$, $T^*=32.1$ (fcc). The $g(r)$'s at fixed pressure were calculated from an average over 200 time steps after a phase transition has occurred (see text) at $H^*=986.5$, $P^*=1800$ (bcc) and $H^*=980.3$, $P^*=1800$ (fcc). Over this time period the average values of ρ^* and T^* were $\rho^*=2.409$, $T^*=32.1$ (bcc) and $\rho^*=2.414$, $T^*=31.4$ (fcc).

ticeably the functions $g_n(r)$. Figure 2 gives a comparison between $g_n(r)$ calculated by a MD simulation at constant energy and constant volume for a perfect fcc (bcc) crystal and $g_n(r)$ calculated by MD simulation at constant enthalpy but variable volume for a fcc (bcc) crystal resulting from a phase change of the system initially placed in a perfect bcc (fcc) structure. There is no appreciable difference between the functions $g_n(r)$ obtained from both simulation methods if the phase structure, density, and temperature are the same. This indicates that the crystals obtained in the phase change are nearly perfect.

The characterization of the evolution of the system by the $g_n(r)$ functions has been completed by analyzing the modification of the number of atoms in the first few neighboring shells of a given atom. The number of atoms in the five first neighboring shells of each atom j of the system was calculated, as a function of time, in the following way. For a given time t, knowing the density $\rho(t)$ of the system, one can calculate the nearest-neighbor distances $d_i(t)$ $(1\leq i\leq 5)$ in the fcc, bcc, and hcp lattices. Setting $d_0(t)\equiv 0$ and $\Delta d_i=(d_{i+1}-d_i)/2$, an atom is considered to be in the ith nearest-neighbor shell of atom j, if its distance to atom j is located between $d_i-\Delta d_{i-1}$ and $d_i+\Delta d_i$. One then obtains the number $n_j^i(t)$ of atoms in the ith shell surrounding atom j. The atom j is considered to belong to a fcc, bcc, or hcp crystal inasmuch as the numbers $n_j^i(t)$ are sufficiently close to those corresponding to one of the preceding structures. At the very high densities of solid ^{4}He at 300 K the differences $d_{i+1}-d_i$ are of the order of 0.2σ, whereas the atomic displacements from their equilibrium positions are of the order of 0.1σ. It can thus happen that, at a given time t, an atom belonging on the average to the ith nearest-neighbor shell of atom j is in fact closer to atom j than some atoms of shell $i-1$. Despite these ambiguities, due to the instantaneous character of $n_j(t)$, we show in Tables I and II, that during a fcc-bcc or a bcc-fcc transition, the evolution of the number of atoms belonging to either a fcc or a bcc crystal corresponds to that of the $g_n(r)$ functions given in Figs. 3 and 4. Tables I and II also show that the vectors **a**, **b**, **c**, and their relative angles vary in accord with the $g_n(r)$ functions. In addition, we calculated as a function of time the values of the angles between the vectors joining atom j to its first-nearest neighbors and verified the appearance (or disappearance) of the angle $\pi/2$ characteristic of the fcc lattice during the bcc-fcc (or fcc-bcc) transition.

In conclusion, from the $g_n(r)$ function it is possible to follow the evolution of the system between different phases or, on the contrary, to ascertain the stability of the initial state. The variations of this function correspond, for the systems studied in the present work, to transitions between nearly perfect crystal states or between a perfect crystal and a fluid state.

The constant-enthalpy—constant-pressure MD simulations have been performed for a system of 432 atoms interacting via the HFDHE2 (Hartree-Fock dispersion) potential of Ref. 7, truncated at a distance $r=2.3\sigma$, for

TABLE I. Evolution of the lengths and relative angles of the vectors **a**, **b**, **c** defining the volume of the system with number of integration time steps during a bcc-fcc transition. The reduced pressure is $P^*=1800$, the reduced enthalpy $H^*=980.3$. $n_{\rm bcc}$ and $n_{\rm fcc}$ denote the number of atoms of "type" bcc and type fcc as defined in Sec. II. In the initial state the vectors **a**, **b**, **c** are along the [100] [010], and [001] directions of the bcc crystal.

Time/Δt	$n_{\rm bcc}$	$n_{\rm fcc}$	$\lvert\mathbf{a}\rvert$	$\lvert\mathbf{b}\rvert$	$\lvert\mathbf{c}\rvert$	θ_{ab}	θ_{ac}	θ_{cb}
1000	294	5	5.63	5.65	5.64	90°	89°	90°
1500	244	48	5.32	5.46	6.18	90°	90°	90°
2000	195	185	5.08	5.26	6.63	89°	89°	90°
2500	200	205	5.03	5.31	6.70	89°	90°	90°
3000	153	184	5.06	5.30	6.68	89°	89°	90°

TABLE II. Same as in Table I for a fcc-bcc transition, $P^*=1800$, $H^*=998.4$. In the initial state the vectors **a**, **b**, and **c** were along the directions [110], [$\bar{1}$10], and [001] of the fcc crystal.

Time/Δt	n_{bcc}	n_{fcc}	$\lvert\mathbf{a}\rvert$	$\lvert\mathbf{b}\rvert$	$\lvert\mathbf{c}\rvert$	θ_{ab}	θ_{ac}	θ_{cb}
0	0	432	5.02	5.02	7.12	90°	90°	90°
600	187	106	4.90	4.92	7.42	89°	90°	90°
1100	195	68	4.92	4.90	7.42	89°	90°	90°
1600	235	40	4.83	4.91	7.71	101°	92°	89°
2100	240	20	4.76	4.87	7.98	108°	91°	89°
2600	255	8	4.84	4.82	8.04	109°	91°	91°

pressures $P^*=P\sigma^3/\epsilon=1800$ and 2200 and enthalpies $H^*=H/\epsilon N$ between 960 and 1300. The time step for integration of the equations of motion was $\Delta t=7\times10^{-4}(m\sigma^2/\epsilon)=1.225\times10^{-15}$ s with m equal to the mass of ^{4}He. A conservation of H^* of 10^{-4}–10^{-5} in relative value was obtained over integration times of $10^4\Delta t$. The value of the parameter W entering [cf. Eq. (1)] was taken equal to 20 m.

Tables III and IV summarize the simulation results obtained at $P^*=1800$ and 2200. For each pressure we considered two types of initial states corresponding to perfect fcc or bcc crystals. Depending on the value of H^* the system stays in its initial state or transits to a different solid or a fluid phase.

If a transition takes place, the variation of $g_n(r)$ and of the vectors **a**, **b**, **c** shows that it occurs in about $1000\Delta t$ (cf. Fig. 1 of Ref. 4). Outside the time intervals over which the transitions take place, the $g_n(r)$ functions correspond to well-defined phases. For certain values of H^*, for instance, $H^*=993$ at $P^*=1800$, the system evolves rapidly from one phase to the other so that it is difficult to assess in which phase the system is at a given time. In this case one cannot exclude the possibility of quasi-equilibrium between two microcrystals each in one of the two phases. Except for this unfavorable case, it is possible to determine, in the time interval over which $g_n(r)$ remains stable (provided it is sufficiently long), the values of the temperature and average volume of the fcc, bcc, or fluid phases in which the system happens to be. From these the equation of state H^* as a function of T^* at fixed pressure results. It is given in Fig. 5. The essential feature is that in each phase H^* is a linear function of T^*, the coefficient of T^* being the same, within statistical uncertainty, in the two solid phases.

At fixed P^*, for increasing values of H^* an initial state corresponding to a fcc crystal gets progressively unstable in the sense that it exists only over time intervals smaller or equal to $1000\Delta t$ as, for instance, for $H^*=1160$, 1154 at $P^*=2200$ and for $H^*=998.4$, 995, 993 at $P^*=1800$. A similar behavior is observed for an initial bcc phase for decreasing values of H^* ($H^*<1136$ at $P^*=2200$ or

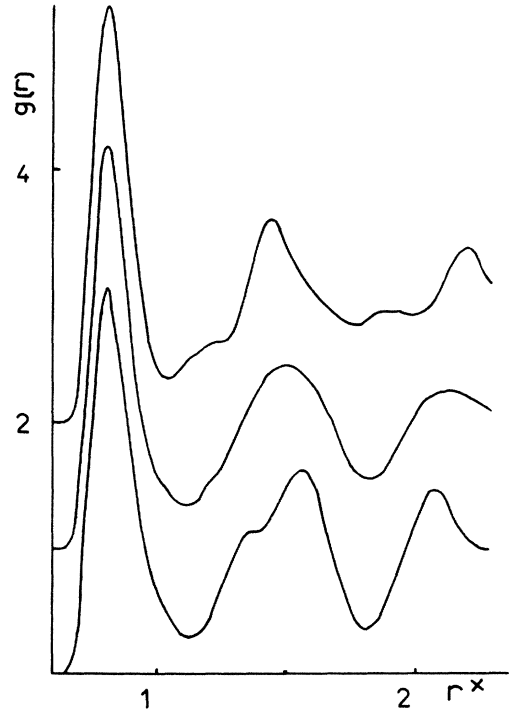

FIG. 3. Evolution of the function $g_n(r)$ ($n=50$) during a bcc-fcc transition ($H^*=980.3$, $P^*=1800$). From bottom to top $g_n(r)$ corresponds to time steps 1000, 1500, and 2000, respectively (cf. Table I).

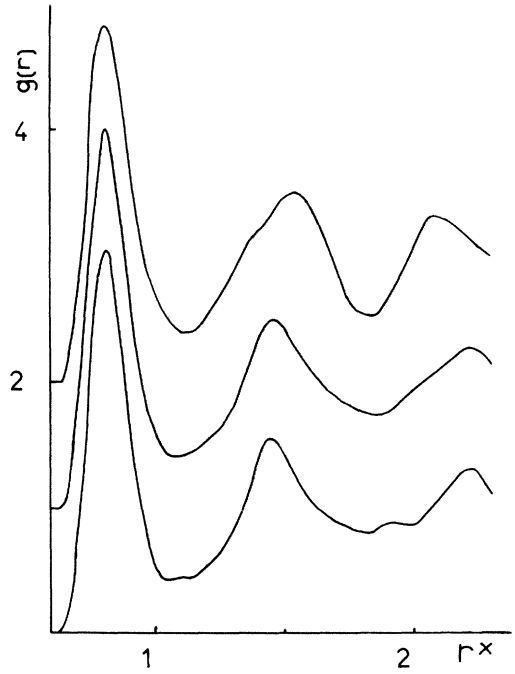

FIG. 4. Same as in Fig. 3 for a fcc-bcc transition ($H^*=998.4$, $P^*=1800$) and time steps (from bottom to top) 600, 1600, and 2100 (cf. Table II).

TABLE III. Equation of state at pressure $P^* = 1800$ calculated by MD at constant pressure and constant enthalpy H^*. The symbols in column 2 denote the nature of the initial configuration of each run (L, liquid; fcc crystal; bcc crystal). Columns 3–5 give the integration time steps at which a transition starts to take place. Typically, a solid-solid transition accomplishes in 1000 time steps, the solid-liquid transition in 2000–3000 time steps. The numbers in parentheses indicate that the evolution of the system from one phase to the other is very rapid or followed by the reverse evolution after a time duration too short to give a precise estimate of the density and, especially, the temperature of the intermediate phase. In this case the values for ρ^* and T^* in columns 6–11 are given in parentheses or omitted. The precision on ρ^* is ± 0.001, and on T^* is ± 0.1. n_t denotes the total number of time steps of the run and P^*_{virial} is the pressure calculated from the virial theorem.

H^*	Initial state	Time of onset of fcc-bcc transition	Time of onset of bcc-fcc transition	Time of onset of solid-liquid transition	n_t	ρ^*_{bcc}	T^*_{bcc}	ρ^*_{fcc}	T^*_{fcc}	ρ^*_{liq}	T^*_{liq}	P^*_{virial}
1036.09	L				3500					2.327	39.1	1799
1028.99	L				2900					2.337	37.1	1799
1024.2	L				3500					2.344	36.0	1799
1019.2	fcc			200	2000					(2.35)	(35.0)	1798
1013.4	L				10 000					2.358	32.7	1793
1004.0	L				5500					2.370	30.1	1800
1002.5	bcc				3200	2.387	36.3					1799
998.4	fcc	< 500			8000	2.393	35.3	2.393	(36.1)			1800
995.4	L				14 000					2.382	27.9	1800
995.0	fcc	< 500			4600	2.397	34.4					1800
993.3	bcc				3300	2.400	33.9					1799
993.3	fcc	(900),(4000)	(2000),(7000)		15 500	(2.400)	(33.2)	2.400	34.8			1801
986.5	fcc	6700			21 200	2.409	31.9	2.410	32.8			1800
986.4	bcc				13 300	2.409	31.9					1800
984.1	fcc	(1000),(2800)	(2000),(3800)		10 850			2.414	32.1			1800
983.9	bcc				6500	2.413	31.2					1800
981.0	bcc	(10 500)	(10 000)		17 200	2.417	30.4					1800
981.0	fcc				9500			2.418	31.2			1800
980.3	bcc		1500		8300	2.418	30.1	2.418	31.1			1798
978.0	fcc	10 000	23 500		35 000	2.421	29.5	2.422	30.4			1800
977.0	bcc		5000		22 700	2.422	29.0	2.424	30.1			1800

TABLE IV. Equation of state at $P^*=2200$ calculated by MD at constant pressure and enthalpy. The meaning of the symbols is the same as in Table III.

H^*	Initial state	Time of onset of fcc-bcc transition	Time of onset of bcc-fcc transition	n_t	ρ^*_{bcc}	T^*_{bcc}	ρ^*_{fcc}	T^*_{fcc}	P^*_{virial}
1160.0	fcc	2500		7700	2.525	38.1	2.525	38.8	2198
1154.3	fcc	2500		3500	2.533	(36.7)	2.533	37.7	2201
1152.2	fcc	5200		9500	2.534	35.9	2.535	36.8	2200
1149.8	fcc	(1000),(2700)	(1500),(3200)	9500	2.538	(35.6)	2.538	36.3	2201
1144.6	bcc		5000	13000	2.543	33.7	2.545	34.8	2199
1144.5	fcc	2700		4100	2.544	33.7	2.545	34.7	2201
1144.3	fcc			9300			2.545	34.7	2200
1143.3	bcc	(5000)	(4200)	6500	2.545	33.4			2199
1141.6	bcc	(7000)	(6500)	8500	2.547	32.8			2199
1141.6	fcc	1800,(4500)	(3300)	6100	2.547	32.7	2.548	33.9	2201
1141.1	bcc	(2500)	(1500)	7400	2.547	32.7			2199
1140.7	bcc		1900	6500	2.548	32.6	2.549	33.7	2199
1140.5	fcc			6700			2.550	33.5	2199
1139.8	bcc			5700	2.549	32.3			2201
1138.0	bcc			6800	2.551	31.7			2199
1136.5	bcc	(6000)	5500	8900	2.553	31.2			2199
1136.1	bcc	500		10000	2.553	(31.2)	2.555	32.3	2198

$H^*<980$ at $P^*=1800$). Between the two limits of stability, initial fcc or bcc crystal states can give rise to one or more transitions from one crystal state to the other. The transitions from the fcc to the bcc crystal states correspond to an increase of temperature ~ 0.8 (in reduced units) at $P^*=1800$ and ~ 1.0 at $P^*=2200$, i.e., ~ 8 and ~ 10 K, respectively, and occur at quasiconstant density despite a significant change of the volume shape, as can be seen readily from the simulation results at $H^*=977$, 998.4 ($P^*=1800$) and $H^*=1152$, 1136.3 ($P^*=2200$). At constant temperature the enthalpy difference between the fcc and bcc phases is 2.8 (reduced units) for $P^*=1800$ and 3.9 for $P^*=2200$. The enthalpy difference between the fluid phase and the bcc phase is 23.8 at $P^*=1800$.

From the simulation results one can also deduce ρ^* as a function of H^* for each of the three phases and hence ρ^* as a function of T^*. This relation is shown on Fig. 6. The dependence of ρ^* on T^* being almost linear one can estimate the density difference between the phases: ~ 0.006 between the fcc and bcc phases and ~ 0.04 between the bcc and liquid at $P^*=1800$, ~ 0.004 between the fcc and bcc phases at $P^*=2200$ for the domain of temperatures considered $30\leq T^*\leq 39$. From these results one can obtain an estimate of the entropy difference between the different phases provided that thermodynamic equilibrium is achieved between these phases for $P^*=1800$ and 2200 in the temperature domain 30–39. Indeed, at phase equilibrium, the equality of the chemical potentials implies that, at constant pressure, the entropy change is equal to the enthalpy change divided by the temperature at phase equilibrium.

The location of the temperature at which, at constant pressure, the phase transition occurs is not easier to obtain in a constant-enthalpy–constant-pressure simulation than in the more conventional MD or MC methods. As a matter of fact, it would be appropriate to calculate the

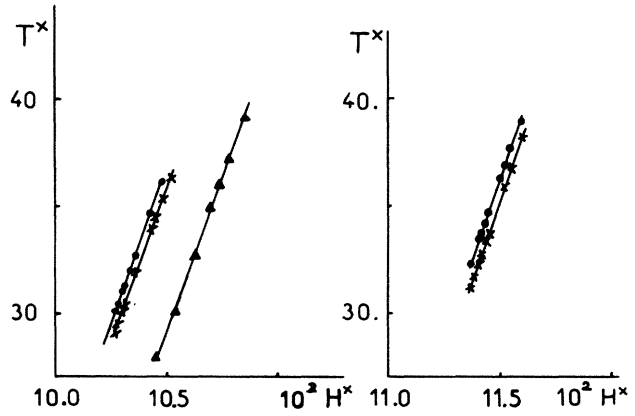

FIG. 5. Equations of state T^* vs H^* at $P^*=1800$ (left) and $P^*=2200$ (right) (dots, fcc phase; crosses, bcc phase; triangles, fluid phase).

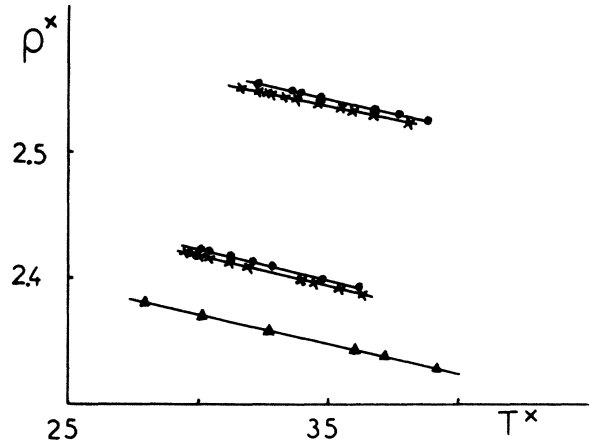

FIG. 6. Equations of state ρ^* vs T^* at $P^*=1800$ (lower curves) and $P^*=2200$ (upper curves). Symbols as in Fig. 5.

free energy by integration of the equation of state starting from a thermodynamic state with known free energy or else to start from a system with known free energy which is transformed by progressive modification of the Hamiltonian into a system of atoms interacting by the Aziz potential.[12] However, one can put forward qualitative arguments allowing an estimate of the transition temperature. In the case of the fcc-bcc transition the simulation results show that the bcc phase exists with good stability only in the temperature domain 30–36 and that for $T^*=32$ and $H^*=985$ its stability is approximately equal to that of the fcc phase. So for this value of $H^*\sim 985$ the fcc and bcc phases appear to be equiprobable in configuration space or also correspond to similar volumes of configuration space and, consequently, have approximately similar entropy. However, since the difference $H^*_{\rm bcc}-H^*_{\rm fcc}$ is positive, at constant P^*, for the phase equilibrium temperature, the entropy of the bcc phase must be higher than that of the fcc phase; therefore the temperature of equilibrium between the bcc and fcc phases of $P^*=1200$ must be higher than 32. On the other hand, it must be less than 36 as the bcc phase gets unstable with respect to the fluid phase above this temperature. A similar argument for $P^*=2200$ leads to the conjecture that, for this pressure, equilibrium between the solid phases can be achieved only for a temperature larger than 34.

Concerning the location of the equilibrium temperature between the solid and liquid phases we remark that, whereas a transition from the solid to the liquid phase is easily obtained, the reverse transition does not seem realizable, at these densities, in simulations of less than 30 000 time steps as evidenced by the run at $P^*=1800$ and $H^*=995$ (cf. Table III). It seems thus not possible to determine the limit of stability of the fluid with respect to the solid when the temperature decreases. The only possible conclusion is that for $P^*=1800$ the solid-liquid equilibrium temperature is lower than ~ 36, the temperature corresponding to the limit of stability of the bcc phase.

From the analysis of the MD results at constant H^* and P^* one also concludes that the existence of a hcp phase is very unlikely for the two pressures and the domain of temperatures considered, with no simulation showing a tendency for transition towards such a phase. The new high-temperature solid phase of solid ^{4}He is thus bcc as discussed already in Ref. 4.

We finally note that although, as shown by Ray,[13] the average pressure calculated from the virial theorem is not equal to P^* if the dynamics of the system derive from the Lagrangian [Eq. (1)], the difference seems smaller than 10^{-3} in relative value for the densities and temperatures considered, (cf. Tables III and IV).

III. MONTE CARLO STUDY

In this section we study the solid-solid and solid-fluid transitions of high-temperature ^{4}He using the Monte Carlo method to sample the isobaric-isothermal ensemble. With this study we want to test the usefulness of the isobaric-isothermal ensemble to characterize the solid-solid transitions, obtain a precise estimate of the volume change between the phases as a function of pressure at fixed temperature, and calculate the differences, of order N^{-1}, between thermodynamic quantities evaluated in different ensembles for systems of finite size.

The extension of the MC method developed by Wood[6] for simulations in the isobaric-isothermal ensemble to the case of a Monte Carlo cell of variable size and shape has already been given by the authors of Ref. 14. The partition function of the isothermal-isobaric ensemble corresponding to the Hamiltonian (2) can be written down easily by remarking, with Andersen,[11] that the isothermal-isobaric ensemble is related to the isoenthalpic-isobaric ensemble in the same way as the canonical ensemble is related to the microcanonical ensemble:

$$\Delta=\frac{C}{N!h^{3N}}\int\prod_{\alpha,\beta=1}^{3}dh_{\alpha\beta}\prod_{j=1}^{N}d\mathbf{s}_j\prod_{i=1}^{N}m^3\det\{\overleftrightarrow{G}\}d\dot{\mathbf{s}}_i\prod_{\alpha,\beta=1}^{3}(W\,d\dot{h}_{\alpha\beta})\exp\left[-\beta\left[\tfrac{1}{2}m\sum_{i=1}^{N}\dot{\mathbf{s}}_i\cdot\overleftrightarrow{G}\cdot\dot{\mathbf{s}}_i+\tfrac{1}{2}W\,\mathrm{Tr}\{\dot{\overleftrightarrow{h}}^t\cdot\dot{\overleftrightarrow{h}}\}\right.\right.$$
$$\left.\left.+P\det\{\overleftrightarrow{h}\}+\sum_{i\,(<j)=1}^{N}v(r_{ij})\right]\right], \tag{5}$$

where C is a constant which makes Δ dimensionless. To take account of the fact that the MD simulations with Lagrangian (1) are subject to the condition $\sum_i\dot{\mathbf{s}}_i=0$ we incorporated the latter condition into the partition function Δ to avoid a systematic difference of order N^{-1} between the thermodynamic properties calculated by the two simulations methods. Then

$$\Delta=\frac{W^9m^{3N}}{N!h^{3N}}C\int\prod_{\alpha,\beta=1}^{3}dh_{\alpha\beta}\prod_{j=1}^{N}d\mathbf{s}_j\prod_{i=1}^{N}d\dot{\mathbf{s}}_i\prod_{\alpha,\beta=1}^{3}d\dot{h}_{\alpha\beta}\delta\left[\sum_{i=1}^{N}\dot{\mathbf{s}}_i\right]\det\{\overleftrightarrow{h}\}^{2N}e^{-\beta H}$$

$$=\frac{W^9m^{3N}}{N!h^{3N}}C\int\prod_{\alpha,\beta=1}^{3}dh_{\alpha\beta}\prod_{j=1}^{N}d\mathbf{s}_j\prod_{i=1}^{N}d\dot{\mathbf{s}}_i\prod_{\alpha,\beta=1}^{3}d\dot{h}_{\alpha\beta}d\mathbf{k}\exp\left[i\mathbf{k}\cdot\sum_{i=1}^{N}\dot{\mathbf{s}}_i\right]\det\{\overleftrightarrow{h}\}^{2N}e^{-\beta H}. \tag{6}$$

Defining $\mathbf{v}_i=\overleftrightarrow{h}\cdot\dot{\mathbf{s}}_i$ and $\mathbf{k}_0=\overleftrightarrow{h}^{-1}\cdot\mathbf{k}$ one obtains

$$\Delta=\frac{W^9 m^{3N}}{N!h^{3N}}C\int\prod_{\alpha,\beta=1}^{3}dh_{\alpha\beta}\prod_{j=1}^{N}ds_j\prod_{i=1}^{N}dv_i\prod_{\alpha,\beta=1}^{3}d\dot{h}_{\alpha\beta}d\mathbf{k}_0\det\{\vec{\mathrm{h}}\}^{N+1}\exp\left[i\mathbf{k}_0\sum_{i=1}^{N}\mathbf{v}_i\right]$$
$$\times\exp\left[-\beta\left[\tfrac{1}{2}m\sum_{i=1}^{N}\mathbf{v}_i^2+\tfrac{1}{2}W\,\mathrm{Tr}\{\vec{\mathrm{h}}'\cdot\vec{\mathrm{h}}\}+P\det\{\vec{\mathrm{h}}\}+\sum_{i(<j)=1}^{N}v(r_{ij})\right]\right]. \quad (7)$$

The integrations on v_i and $\dot{h}_{\alpha\beta}$ are easily performed, as well as the integration on k_0 since the integrand is a Gaussian function of k_0^2. Finally, the partition function takes the form

$$\Delta=\frac{C}{N!}\left[\frac{2\pi W}{\beta}\right]^{9/2}\left[\frac{2\pi m}{h^2\beta}\right]^{3N/2}\left[\frac{2\pi m\beta}{N}\right]^{3/2}\int\prod_{\alpha,\beta=1}^{3}dh_{\alpha\beta}\prod_{j=1}^{N}ds_j\det\{\vec{\mathrm{h}}\}^{N+1}\exp\left[-\beta\left[P\det\{\vec{\mathrm{h}}\}+\sum_{i(<j)=1}^{N}v(r_{ij})\right]\right]. \quad (8)$$

The thermodynamic quantities are obtained as their average value over a sequence of configurations sampled, starting from an initial configuration of bcc or fcc crystal or fluid type, according to the algorithm of Metropolis. For a configuration corresponding to the values s_i^α and $h_{\alpha\beta}$ of the component of s_i and h, the random and *a priori* modification of the variables is made in the domain $s_i^\alpha\pm\Delta s_i^\alpha$ and $h_{\alpha\beta}\pm\Delta h_{\alpha\beta}$. The values of Δs_i^α and $\Delta h_{\alpha\beta}$ which lead to an acceptance ratio 0.5 of the new configuration are $\Delta s_i^\alpha\sim0.02$ and $\Delta h_{\alpha\beta}\sim0.04\sigma$ for the thermodynamic states considered (note that s_i^α is dimensionless and varies between 0 and 1). The ratio between the attempted moves of s_i^α and the attempted changes of the volume is taken equal to N in our calculations. As a matter of fact, for the high densities considered, a more frequent sampling of the volume appears to be statistically significant only if the positions of a sufficiently large number of atoms have changed. With these conditions of sampling of the volume, a phase transition was obtained after several hundred trial moves of the volume.

We have calculated by simulation in the ensemble described above the isotherm $T^*=32$ of a system of $N=432$ atoms interacting by the Aziz potential[7] in the pressure domain 1300–2300. As for the case of the MD simulations at constant enthalpy and pressure, a function $g_n(r)$ can be evaluated, where, obviously, n denotes no longer a number of integration time steps, but a set of successive configurations generated at constant P^* and T^* in configuration space. In the following a value of n corresponds to the configurations generated by $n\times N$ samplings of the variables s_i and therefore, as explained above, to n samplings of the volume. To follow the evolution of the system between different phases we used the value $n=50$. When a transition takes place, the volume changes shape and the density varies. Figure 7 represents, for $P^*=1300$, the variation of the density ρ_n, with $n=50$, as a function of the number of samplings of the volume. The initial state of the system is fcc, the final state is fluid, the intermediate state is bcc. The figure shows that the evaluation of the average densities in the different phases can be obtained with good precision. From the simulations we obtained the equation of state given in Table V and represented in Fig. 8. From Table V it appears that for $P^*=2300$ the initial bcc state evolves towards a fcc state after a sequence of configurations corresponding to $n=2800$, i.e., after 1.2×10^6 displacements of the atoms and 2800 samplings of the volume. At $P^*=1500$ the fcc crystal transforms into a bcc crystal after a sequence of configurations of $n=5500$, at $P^*=1300$ this transformation occurs after a sequence of configurations of $n\sim2000$. At this pressure $P^*=1300$ the bcc phase transits to a fluid phase after a sequence of configurations of $n=2000$ if the initial state was a perfect bcc crystal. The fluid part of the isotherm was determined between $P^*=1200$ and 1600; in this domain the fluid phase is stable over a sequence of configurations of $n\sim15000$.

The simulation results obtained in the isothermal-isobaric ensemble at $T^*=32$ are in good agreement with the MD results for identical thermodynamic states. The density differences between the phases are easily estimated due to the quasiparallelism of the curves P^* as a function of ρ^*. The volume difference is ~0.006 between the solid phases and ~0.04 between the solid and the fluid phases, values identical to those obtained from the MD simulations. However, if the density *differences* between the two solid phases are identical for the two simulation methods, it appears that for identical values of P^* and T^*, the densities are larger by ~0.001 in the isothermal-isobaric ensemble than in the MD simulations. This density increase would have been even more important (~0.003) had the

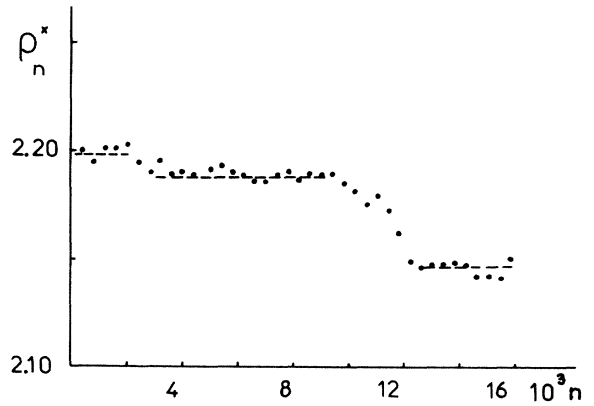

FIG. 7. Evolution of the ρ_n^* ($n=50$, see text) with number of samplings of the volume V in an isothermal-isobaric Monte Carlo simulation at $T^*=32$ and $P^*=1300$. The dashed lines indicate the densities of the (metastable) fcc and bcc phases and of the (stable) liquid phase.

TABLE V. Equation of state at $T^*=32$ calculated by MC in the isothermal-isobaric ensemble. n denotes the total number of configurations generated according to the notations of the text (n samplings of the volume plus $N\times n$ samplings of the atomic positions). Columns 3–5 give the values of n at which the onset of the fcc-bcc, bcc-fcc, or solid-fluid transitions takes place. The meaning of the parentheses is the same as in Tables III and IV. The precision of the densities is typically ±0.001. The virial pressure P^*_{virial} differs from P^* by a term of order N^{-1}.

P^*	Initial state	n fcc-bcc	n bcc-fcc	n solid-fluid	n	ρ^*_{bcc}	ρ^*_{fcc}	ρ^*_{liq}	P^*_{virial}
2300	bcc		2800		4000	2.586	2.591		2299
2200	bcc				2000	2.553			2206
2200	fcc				2000		2.560		2204
2150	bcc	(7800),(12 000)	(7500),(11 200)		16 000	2.536			2154
2000	fcc				2000		2.492		2003
1950	bcc				4000	2.467			1956
1800	bcc				2000	2.412			1805
1780	fcc				4000		2.411		1785
1750	fcc				2000		2.400		1753
1720	bcc				1000	(2.380)			1724
1680	bcc				2000	2.363			1686
1650	fcc				4000		2.359		1655
1600	bcc				2000	2.330			1604
1600	L				11 000			2.284	1605
1500	bcc				2000	2.287			1505
1500	fcc	5500			10 000	2.288	2.295		1505
1500	L				11 000			2.243	1505
1400	bcc				2000	2.242			1405
1400	L				4000			2.198	1403
1300	bcc			2000	6000	2.187		2.149	1302
1300	fcc	2000		10 000	16 000	2.188	2.198	2.147	1308
1200	L				2000			2.098	1202

constraint $\sum_i \dot{\mathbf{s}}_i=0$ not been included in the partition function Δ. The density difference observed in the two simulation methods is a consequence of the finite size of the system. The latter entails differences of order N^{-1} in the thermodynamic quantities calculated in different ensembles. From the only calculations accomplished in this work for the isotherm $T^*=32$ in the isothermal-isobaric ensemble it is not possible to locate the transition plateau. The instability of one solid phase with respect to the other and with respect to the fluid allows one, by a qualitative argument similar to the one presented in the preceding section, to locate the equilibrium between the solid phases between $P^*=1400$ and 2200 and the liquid-solid equilibrium at $P^*>1400$.

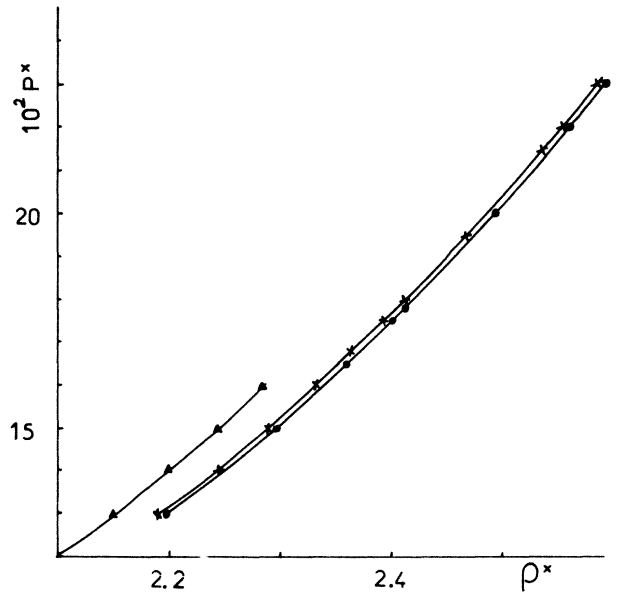

FIG. 8. Equation of state P^* vs ρ^* at $T^*=32$ calculated from an isothermal-isobaric MC simulation. Symbols as in Fig. 5.

In Ref. 15, Frenkel, using a method proposed recently by Frenkel and Ladd[12] to calculate the free energy of a solid, locates the transition pressure of the isotherm $T^*=32$ at 15.07 GPa (i.e., $1776\epsilon/\sigma^3$) for the fluid-fcc transition and at 13.2 GPa ($1556\epsilon/\sigma^3$) for the fcc-bcc transition. As noted in Ref. 15 the results of our calculations in the isothermal-isobaric ensemble are in excellent agreement with those of Ref. 15 obtained in the canonical ensemble. The equilibrium pressures between the phases calculated by Frenkel[15] are also in full accord with the stability domains determined for these phases in the isothermal-isobaric ensemble.

On account of the extremely small free-energy differences between the fcc and bcc solids ($\sim 10^{-3}$) it seems to us that finite-size corrections have to be considered in order to make quantitative comparison with experimental results (cf. differences between the densities calculated in the MD and isothermal-isobaric ensemble).

To summarize briefly this section, we have shown that the isobaric ensemble defined by the partition function Δ can be used advantageously to study solid-solid transitions. The simulations in this ensemble permit a precise estimate of the volume differences between the phases.

The computing times required to give evidence of a phase transition are identical to those needed when the MD method at constant enthalpy and pressure is used.

IV. CONCLUSION

The main conclusion of this study of phase transitions in ^{4}He at high pressure and $T=300$ K lies in the identification of the experimental triple point as an equilibrium between a fluid, a fcc, and a bcc phase. The occurrence of a hcp phase is excluded by our simulation calculations by MD and in the isothermal-isobaric ensemble, with no initial fcc state evolving towards such a phase.

The potential by Aziz *et al.*[7] does not give a completely quantitative description of ^{4}He in the pressure domain 10—20 GPa and temperatures of the order ~ 300 K. Our simulation results and those of Frenkel[15] indicate that the values for the melting pressures and temperatures calculated with this potential are in excess by 10—15 %, the fluid-fcc-bcc triple point being located at a temperature higher than 330 K. A modification of the repulsive part of the potential by Aziz *et al.*[7] reduces these discrepancies.[1,4] Inclusion of three-body forces in the interaction potential and of quantum corrections could necessitate a further readjustment of the parameters to maintain quantitative agreement between the theoretical and experimental equations of state. At the pressures considered the three-body contributions to the pressure are estimated to be ~ 0.4 GPa (Ref. 4); and the quantum corrections to the pressure ~ -0.3 GPa (Ref. 15).

We finally would like to describe several modes of transformation of the parallelepiped defined by the vectors **a**, **b**, **c** in the course of the solid-solid transition. In Table I an example is given of a transformation from a bcc to a fcc crystal during a molecular-dynamics simulation. Initially the vectors **a**, **b**, **c** are along the [100], [010], and [001] directions of the bcc crystal and the lengths $|\mathbf{a}|$, $|\mathbf{b}|$, $|\mathbf{c}|$ correspond to 6 times the distance between second-nearest-neighbor atoms. In the transformation the cubic volume containing the 432 atoms of the system becomes a rectangular parallelepiped with quadratic section in the plane perpendicular to **c**. The lengths $|\mathbf{a}|$, $|\mathbf{b}|$, and $|\mathbf{c}|$ evolve in a way such that the ratios $|\mathbf{c}|/|\mathbf{a}|$ and $|\mathbf{c}|/|\mathbf{b}|$ vary from 1 to $\sim\sqrt{2}$. This kind of transformation has been observed, for instance, in Refs. 5 and 14 and corresponds to the deformation of the rectangle constituted by an atom and its four-nearest neighbors in the $(1\bar{1}0)$ plane of the bcc crystal into a square constituted by an atom and its four nearest neighbors in a (100) plane of the fcc crystal. This transformation can be accomplished by keeping the angles between **a**, **b**, and **c** fixed.

Table II corresponds to an example of a transformation of a fcc crystal into a bcc crystal. Initially the vectors **a** and **b** are along the [110] and $[\bar{1}10]$ directions of the fcc crystal. During the transition they become the $[11\bar{1}]$ and $[\bar{1}11]$ directions of the bcc crystal and consequently the angle between **a** and **b**, θ_{ab} changes from 90° to $\sim\arccos(-\frac{1}{3})=109°$. The **c** axis initially along the [001] direction of the fcc crystal becomes the [101] direction of the bcc crystal and the ratios $|\mathbf{c}|/|\mathbf{a}|$ and $|\mathbf{c}|/|\mathbf{b}|$ vary from $\sqrt{2}$ (ratio of the second-nearest-neighbor distance to the first-nearest-neighbor distance in the fcc crystal) to about $2\sqrt{(2/3)}$ (ratio of the third-nearest-neighbor distance to the first-nearest-neighbor distance in the bcc crystal).

It seems thus possible during a phase transition to follow the evolution of the crystal by analyzing the modifications of the lengths and relative angles of the vectors **a**, **b**, and **c**. However, we can remark that nothing opposes the vectors **a**, **b**, **c** to orient, during the dynamical evolution of the system, along an arbitrary direction of the crystal lattice. We give an example for a crystal transiting from a fcc to a bcc phase and then again to a fcc phase. In the initial fcc state the vectors **a**, **b**, and **c** were along the directions [110], $[\bar{1}10]$, and [001] of the crystal having lengths 4.9, 4.9, and 7.10, respectively. In the bcc phase the vectors **a**, **b**, and **c** were along the directions [111], $[\bar{1}11]$, and $[1\bar{1}1]$ with lengths 4.9, 4,9, and 8.1, respectively, in accord with the type of transformation described above. From this bcc phase the system evolved again to a fcc phase, the vectors **a**, **b**, **c** having typically components (4.93, 2.12, 0.53), (−0.63, 4.22, −0.53), and (0.64, 0.91, 8.01) corresponding to $\theta_{ab}\sim 76°$, $\theta_{bc}\sim 90°$ and $\theta_{ac}\sim 77°$ and moduli 5.39, 4.30, 8.09. The determination of the crystal directions of **a**, **b**, and **c** is less easy for this case than for the transitions described in Tables I and II, indeed the directions of **a**, **b**, and **c** are, respectively, $[5\bar{3}0]$, [110], and $[1\bar{1}6]$. Therefore it is important to remark that for successive transitions with substantial modifications of the orientations and lengths of the vectors **a**, **b**, **c** the evolution of the system can be followed only by resorting to correlation functions, of which $g_n(r)$ is an example.

ACKNOWLEDGMENTS

The calculations on the Cray-1S at Ecole Polytechnique (Palaiseau) were made possible by the Conseil Scientifique du Centre de Calcul Vectoriel pour la Recherche. The Laboratoire de Physique Théorique et Hautes Energies and Physique des Milreux trés Condensés are "Laboratoires associés au Centre National de la Recherche Scientifique."

[1] P. Loubeyre, J. M. Besson, and J. P. Hansen, Phys. Rev. Lett. **49**, 1172 (1982).

[2] P. Loubeyre and J. P. Hansen, Phys. Rev. B **31**, 634 (1985).

[3] P. Loubeyre, D. Levesque, and J. J. Weis, Phys. Rev. B **33**, 318 (1986).

[4] D. Levesque, J. J. Weis, and M. L. Klein, Phys. Rev. Lett. **51**, 670 (1983).

[5] M. Parrinello and A. Rahman, Phys. Rev. Lett. **45**, 1196 (1980).

[6] W. W. Wood, *Physics of Simple Liquids*, edited by H. N. V.

Temperley, J. S. Rowlinson, and G. S. Rushbrooke (North-Holland, Amsterdam, 1968).
[7]A. A. Aziz, V. P. Nain, J. S. Carley, W. L. Taylor, and G. T. McConville, J. Chem. Phys. **70**, 4330 (1979).
[8]M. H. Kalos, M. A. Lee, P. A. Whitlock, and G. V. Chester, Phys. Rev. B **24**, 115 (1981).
[9]M. Parrinello and A. Rahman, J. Appl. Phys. **52**, 7182 (1981).
[10]S. Nosé and M. L. Klein, J. Chem. Phys. **78**, 6928 (1983).
[11]H. C. Andersen, J. Chem. Phys. **72**, 2384 (1980).
[12]D. Frenkel and A. J. C. Ladd, J. Chem. Phys. **81**, 3188 (1984).
[13]J. A. Ray, J. Chem. Phys. **79**, 5128 (1983).
[14]S. Yashanath and C. N. R. Rao, Mol. Phys. **54**, 245 (1985); R. Najafabadi and S. Yip, Scr. Metall. **17**, 1199 (1983).
[15]D. Frenkel, Phys. Rev. Lett. **56**, 858 (1986).